Visual perceptual learning modulates decision network in the human brain: The evidence from psychophysics, modeling, and functional magnetic resonance imaging

Ke Jia
School of Psychological and Cognitive Sciences and Beijing Key Laboratory of Behavior and Mental Health, Peking University, Beijing, China
PKU-IDG/McGovern Institute for Brain Research, Peking University, Beijing, China
Key Laboratory of Machine Perception (Ministry of Education), Peking University, Beijing, China

Xin Xue
Department of Health Industry Management, Beijing International Studies University, Beijing, China
School of Psychological and Cognitive Sciences and Beijing Key Laboratory of Behavior and Mental Health, Peking University, Beijing, China
PKU-IDG/McGovern Institute for Brain Research, Peking University, Beijing, China
Key Laboratory of Machine Perception (Ministry of Education), Peking University, Beijing, China

Jong-Hwan Lee
Department of Brain and Cognitive Engineering, Korea University, Seoul, Republic of Korea

Fang Fang
School of Psychological and Cognitive Sciences and Beijing Key Laboratory of Behavior and Mental Health, Peking University, Beijing, China
PKU-IDG/McGovern Institute for Brain Research, Peking University, Beijing, China
Key Laboratory of Machine Perception (Ministry of Education), Peking University, Beijing, China
Peking-Tsinghua Center for Life Sciences, Peking University, Beijing, China

Jiaxiang Zhang
School of Psychology, Cardiff University, Cardiff, UK

Sheng Li
School of Psychological and Cognitive Sciences and Beijing Key Laboratory of Behavior and Mental Health, Peking University, Beijing, China
PKU-IDG/McGovern Institute for Brain Research, Peking University, Beijing, China
Key Laboratory of Machine Perception (Ministry of Education), Peking University, Beijing, China

Citation: Jia, K., Xue, X., Lee, J.-H., Fang, F., Zhang, J., & Li, S. (2018). Visual perceptual learning modulates decision network in the human brain: The evidence from psychophysics, modeling, and functional magnetic resonance imaging. *Journal of Vision*, *18*(12):9, 1–19, https://doi.org/10.1167/18.12.9.

https://doi.org/10.1167/18.12.9 Received March 12, 2018; published November 15, 2018 ISSN 1534-7362

Perceptual learning refers to improved perceptual performance after intensive training and was initially suggested to reflect long-term plasticity in early visual cortex. Recent behavioral and neurophysiological evidence further suggested that the plasticity in brain regions related to decision making could also contribute to the observed training effects. However, how perceptual learning modulates the responses of decision-related regions in the human brain remains largely unknown. In the present study, we combined psychophysics and functional magnetic resonance imaging (fMRI), and adopted a model-based approach to investigate this issue. We trained participants on a motion direction discrimination task and fitted their behavioral data using the linear ballistic accumulator model. The results from model fitting showed that behavioral improvement could be well explained by a specific improvement in sensory information accumulation. A critical model parameter, the drift rate of the information accumulation, was correlated with the fMRI responses derived from three spatial independent components: ventral premotor cortex (PMv), supplementary eye field (SEF), and the fronto-parietal network, including intraparietal sulcus (IPS) and frontal eye field (FEF). In this decision network, we found that the behavioral training effects were accompanied by signal enhancement specific to trained direction in PMv and FEF. Further, we also found direction-specific signal reduction in sensory areas (V3A and MT+), as well as the strengthened effective connectivity from V3A to PMv and from IPS to FEF. These findings provide evidence for the learning-induced decision refinement after perceptual learning and the brain regions that are involved in this process.

Introduction

Training can induce behavioral improvements in perceptual sensitivity (Gilbert, Sigman, & Crist, 2001; Sagi & Tanne, 1994; Sasaki, Nanez, & Watanabe, 2010; Shibata, Sagi, & Watanabe, 2014; Watanabe & Sasaki, 2015). However, the underlying neural mechanism of this training effect remains highly controversial. Early psychophysical studies proposed a sensory modification hypothesis and showed that the enhanced perceptual performance is mostly specific to the trained location, feature, or eye, indicating plastic changes in the early sensory cortices (Ahissar & Hochstein, 1997; Ball & Sekuler, 1987; Fahle, 1997; Fahle & Morgan, 1996; Fiorentini & Berardi, 1980; Karni & Sagi, 1991). Later psychophysical studies, on the other hand, provided the evidence that the specificity is not an inherent property of perceptual learning as it can be eliminated by a double training procedure (Xiao et al., 2008; Zhang et al., 2010; see also Hung & Seitz, 2014; Liang, Zhou, Fahle, & Liu, 2015a, 2015b; Zhang & Yu, 2016 for active debates on this issue). It is also suggested that the specificity itself is also insufficient to support the sensory modification hypothesis, concerning that the specificity of perceptual learning may also originate from the local idiosyncrasies of the retinal image or the hierarchical structure of information flow in the visual system (Dosher, Jeter, Liu, & Lu, 2013; Dosher & Lu, 1998; Mollon & Danilova, 1996; Petrov, Dosher, & Lu, 2005). The physiological and neuroimaging studies that directly tested the sensory modification hypothesis yielded inconsistent results (Adab & Vogels, 2011; Crist, Li, & Gilbert, 2001; Hua et al., 2010; Jehee, Ling, Swisher, van Bergen, & Tong, 2012; Shibata et al., 2012; Yan et al., 2014; Yotsumoto, Watanabe, & Sasaki, 2008; Yu, Zhang, Qiu, & Fang, 2016). For instance, training on an orientation discrimination task changed neural response profile in V1 that favored the sensory modification hypothesis (Schoups, Vogels, Qian, & Orban, 2001), whereas comparable learning effects in behavior were only accompanied by weak changes in sensory areas in other studies (e.g., Ghose, Yang, & Maunsell, 2002). Although learning was found to exert larger influence on V4 than V1, whether this change of activity was driven by neural populations preferring the trained orientation (T. Yang & Maunsell, 2004) or the most informative neurons (Raiguel, Vogels, Mysore, & Orban, 2006) remains controversial.

The inconsistency concerning the sensory modification hypothesis raised the possibility for an alternative explanation, which proposed that perceptual learning is associated with the enhancement in the readout of sensory inputs and the modification of the neural activity in higher level decision-making areas (Dosher et al., 2013; Dosher & Lu, 1998; Petrov et al., 2005). This idea is evidenced by single-unit recording in primates showing that training changes neural activity in decision-making areas (lateral intraparietal cortex, LIP) rather than in sensory cortex (middle temporal area, MT; Law & Gold, 2008, 2009). Similarly, neuroimaging studies in human (Kahnt, Grueschow, Speck, & Haynes, 2011) showed that training changed neural representations of the decision variables in anterior cingulate cortex.

To reconcile these empirical findings, theoretical models that suggested multiple mechanisms in perceptual learning have been proposed. For example, Watanabe and Sasaki (2015) proposed a two-stage model that constitutes a feature-based plasticity and a task-based plasticity. In their model, the feature-based plasticity represents the learning-induced changes in sensory feature representations, while the task-based plasticity accounts for other changes in task-related processing. The two forms of plasticity jointly contribute to the observed learning effects. More recently, Maniglia and Seitz (2018) have proposed another

model that emphasizes the joint contribution of different brain systems to the learning effect. These systems range from low-level sensory representation to higher level cognitive processing, which could be mediated by the type of training task and individual differences. Both models suggested the importance of the high-level mechanisms beyond sensory processing in perceptual learning. Perceptual decision is the process that transfers sensory information into behavioral actions. It is known to be a complex function that is mediated by a network consisting of separate but interacting processes (Gold & Shadlen, 2007; Heekeren, Marrett, & Ungerleider, 2008). Therefore, fully understanding perceptual learning would inevitably require the examination of the training effects on decision process.

It is well known that perceptual decision can be decomposed using a series of sequential sampling models (Bogacz, Brown, Moehlis, Holmes, & Cohen, 2006; Ratcliff & McKoon, 2008). In these models, the evidence for each response alternative is accumulated over time, and the response is made when one of the accumulators reaches the decision threshold. Recent psychophysical studies in perceptual learning fitted the decision-making models to behavioral data, showing that training mainly improved the quality of the sensory evidence to the decision accumulator (Dutilh, Vandekerckhove, Tuerlinckx, & Wagenmakers, 2009; C. C. Liu & Watanabe, 2012; Petrov, Van Horn, & Ratcliff, 2011; Zhang & Rowe, 2014). These investigations have made an initial attempt to quantitatively measure the contribution of the refined decision process to the improved perceptual sensitivity. More importantly, decomposing the behavioral data into single trial model parameters enabled us to localize the decision-making network in human brain (Eichele et al., 2008; van Maanen et al., 2011) and to systemically investigate the training effects within this network.

In the present study, we used a linear ballistic accumulator (LBA) model to identify the changes in the decision process before and after training on a motion direction discrimination task (Ball & Sekuler, 1987; Chen et al., 2015; Jia & Li, 2017). The model assumes a linear accumulation-to-threshold process governing the perceptual decision process (Brown & Heathcote, 2008; Donkin, Brown, & Heathcote, 2011). By correlating the parameter of LBA model with the recorded functional magnetic resonance imaging (fMRI) data, we searched for the brain network that covaried with the decision parameters on a trial-by-trial basis. Our results showed that, perceptual training facilitates information accumulation of the decision process by modifying the stimuli representation in the sensory areas, enhancing the activity in decision areas, and strengthening the feedforward connection between them.

Materials and methods

Subjects

Twenty-two subjects (10 males, 12 females; age range: 17–25 years) completed the experiment. All participants had normal or corrected-to-normal vision and were naïve to the purpose of the experiment. All participants gave written informed consent. The study was approved by the local ethics committee.

Stimuli

The stimuli (dynamic random dot displays, DRDs) were displayed on a cathode ray tube monitor (CRT, 40-cm horizontally wide; resolution, 1,024 × 768; refresh rate, 60 Hz) in the behavioral sessions and via a liquid crystal display (LCD) projector (48-cm horizontally wide; resolution, 1,024 × 768; refresh rate, 60 Hz) during the fMRI sessions. Psychtoolbox 3.0 (Brainard, 1997; Pelli, 1997) in the MATLAB (MathWorks, Natick, MA) environment was used to generate and display the stimuli. Each participant viewed the stimuli binocularly at a distance of 75 cm from the screen.

To generate a DRD, we randomly generated a set of dots, which was presented for one frame and replaced by another set of dots with a constant positional offset (Britten, Shadlen, Newsome, & Movshon, 1992). All DRDs were presented in an invisible 10° diameter aperture centered on the black background (~0 cd/m^2). At any one moment, 400 dots within an aperture moved in the same direction at a speed of 4°/s. The dots that moved out of the aperture reappeared at the opposite side of the aperture to conserve the dot density.

Procedure

The experiment adopted a motion direction discrimination task (Huang, Lu, Tjan, Zhou, & Liu, 2007) and consisted of a pretest phase (two days), a training phase (10 days), and a posttest phase (two days; Figure 1A). The procedure for a typical trial is shown in Figure 1B. At the beginning of each trial, a red reference cross was presented for 500 ms. The orientation of the long arm of the red cross served as the reference direction for the upcoming DRD. The reference cross was followed by a red fixation point that

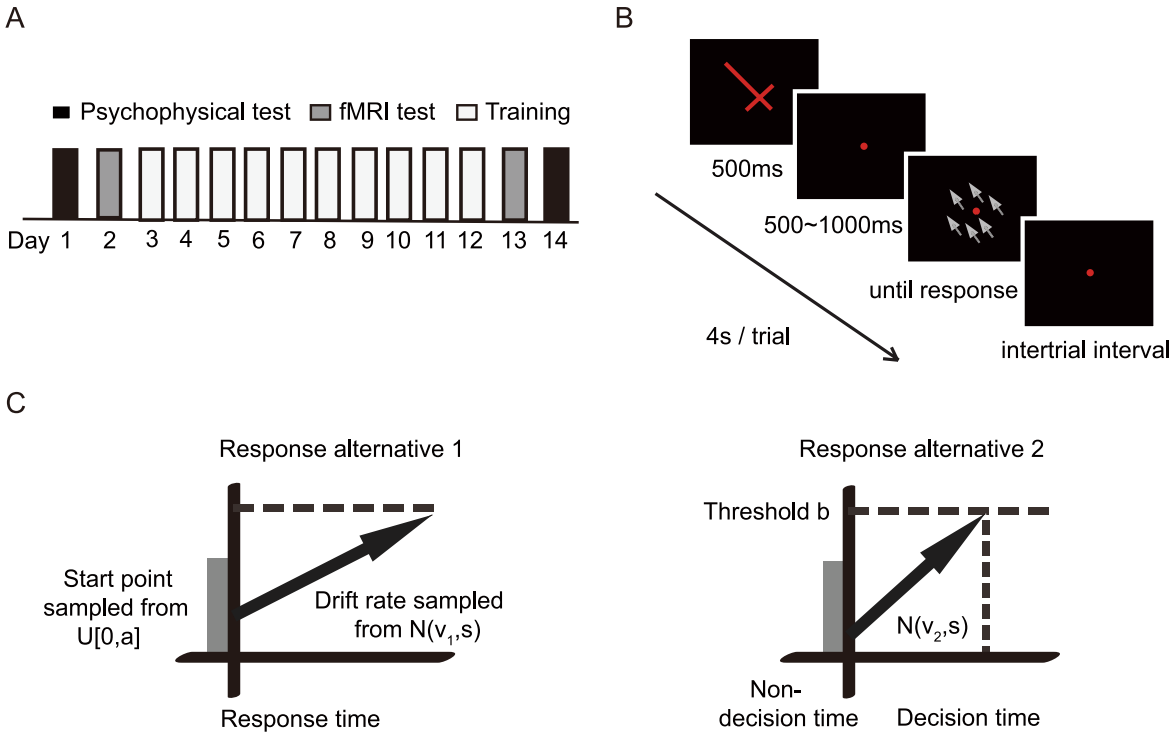

Figure 1. Schematic illustrations of the experimental design and LBA model. (A) Experimental procedure. Participants were trained with the motion direction discrimination task for 10 days. Before and after the training phase, the performance of the direction discrimination task was measured both inside and outside the MRI scanner with a fixed angle difference (4°). (B) Motion direction discrimination task. For each trial, the participants were instructed to report whether the direction of the motion stimulus was clockwise or counterclockwise relative to the orientation of the long arm of the red cross. (C) LBA model. The model assumed one accumulator for each decision option, and each accumulator gathers evidence independently with a fixed drift rate *v*. Decision is made once the response threshold of one accumulator is reached.

remained visible during the whole trial. After a random delay between 500 and 1,000 ms, the DRD was presented for 1,500 ms or until participants made a response. The participants were asked to report whether the direction of the DRD was clockwise or counterclockwise relative to the orientation of the long arm of the reference cross by pressing one of two keys. The duration of the whole trial was set to 4 s. We had the stimulus duration varied across trials based on RT to ensure that the fMRI signal related to information accumulation was not affected by losing sensory input (e.g., fixed shorter duration) or adding extra sensory input after decision process (e.g., fixed longer duration).

Before the pretest phase, each participant practiced 80 trials of the motion direction discrimination task (angle difference = 8°) to familiarize themselves with the task. After the practice, a baseline performance of the direction discrimination task (angle difference = 4°, defined by a pilot study; four blocks and 30 trials for each direction in each block) along 45° and 135° (90° represented vertical up) was measured for each participant. The range of baseline accuracy for all the participants was between 60% and 85%. The pretest phase in the second day was conducted inside the scanner. Each participant completed four runs of the direction discrimination task. Each run consisted of 60 task trials (30 trials along 45° and 30 trials along 135°) and 15 fixation trials, in which the participants were required to fixate at the red fixation point for 4 s without any response. The order of these trials was pseudorandomized for each run and each participant, except that the first two trials and the last three trials in each run were the fixation trials. Functional localizers were conducted in the same session (see ROI definition).

The training phase outside the scanner lasted for 10 days to ensure the saturation of the learning effect. The participants completed 10 runs each day (60 task trials and 10 fixation trials per run), and each training session lasted for approximately 1 hr. The initial angle difference of the training was 4°, and the angle difference was fixed for each training session. Once the task accuracy reached above 79.4%, the task difficulty increased in the next day along the predetermined options (i.e., 3°, 2°, 1.5°, and 1°). We adopted this training protocol, rather than the multiple staircases method or constant stimuli method, to obtain more

difficult trials throughout the training (Hung & Seitz, 2014; Thompson, Tjan, & Liu, 2013). The participants were randomly divided into two groups. Half of the participants were trained along 45°, and the other half were trained along 135°. Auditory feedback was given upon incorrect responses during the training. A visual feedback of "slow down" or "hurry up" was presented when the response time was faster than 250 ms or slower than 1,500 ms, respectively.

The procedure of the posttest phase was identical to the pretest phase, except for the order of the measurements (fMRI session was ahead of behavioral session). To note here, the main purpose of the current study was to define the drift rate related decision network and investigate the training effect in this network. Therefore, we equated the stimuli by using the same angle difference for the trained and untrained directions both before and after training, ensuring that the only difference across conditions was training. Task difficulty is less likely to be a confounding factor in this design, as previous studies using similar stimuli showed no systematic change of BOLD signals across various angle differences (Na, Bi, Tjan, Liu, & Fang, 2018).

fMRI data acquisition

Echo planar imaging (EPI) and T1-weighted anatomical data ($1 \times 1 \times 1$ mm^3) were collected from a Siemens Trio 3T scanner with a 12-channel phase-array coil. EPI data (gradient echo-pulse sequences) were acquired from 33 axial slices (whole brain coverage; repetition time: 2,000 ms; echo time: 30 ms; flip angle: 90°; resolution: $3 \times 3 \times 3$ mm^3; scanning order: interleaved increase).

Data analysis

Behavioral data analysis

The behavioral data measured inside the scanner were analyzed. Trials with a response time (RT) less than 250 ms or greater than 1,500 ms were removed from the analysis to ensure that the measured RTs were produced from a single decision process (Ratcliff & McKoon, 2008). The removed trials were less than 5% for 20 participants and 5%–10% for the other two participants. A repeated measures ANOVA on discrimination accuracy and RT, training group (45° vs. 135°) × motion direction (trained vs. untrained) × session (pretest vs. posttest), did not reveal any significant effect of training group (see Supplementary Figure S1). Therefore, the data from the two training groups were combined for further analyses.

Single-trial LBA model

The LBA model (Figure 1C) is a simplified but complete version of the sequential sampling model that can be used to estimate single trial parameters (Brown & Heathcote, 2008). For each trial, the model assumes that the decision information for each response alternative is accumulated by an independent accumulator at a constant speed (drift rate $\hat{v}$; sampled from a normal distribution with mean value v and deviation of the drift rate across trials, s). The decision information is accumulated from a start point ($\hat{a}$, sampled from a uniform distribution U[0 a]), which represents the response bias. A response is made when one of the accumulators reaches the response threshold (b). The decision caution was defined as the information needed to be accumulated, i.e., $b - a/2$. The model also took into account the time used for the sensory process before the decision-making and the motor execution after decision-making. The nondecision time is termed as t_0. Therefore, the reaction time of each trial can be calculated as $(b - \hat{a})/\hat{v} + t_0$. With the LBA model, we can obtain a set of parameters (a, b, v, s, t_0) for each participant and each condition that best fits the reaction time distributions both in the correct and incorrect trials.

Behavioral data from the fMRI sessions were fitted using the LBA model with the methods of Bayesian estimation. Specifically, for each participant, behavioral data (accuracy and RT for all trials) were split into four groups, motion direction (trained vs. untrained) × session (pretest vs. posttest), and viewed as the evidence in the process of Bayesian estimation. We specified a uniform prior distribution for each parameter (a, b, v, s, t_0) and assumed that the parameters of the two accumulators were the same, except that the summation of the drift rate of the two accumulators was set to 1 to scale the estimated parameters. To examine which model parameters can account for the training-induced performance change across the four conditions (motion direction × session), we constructed 31 LBA models that consisted of all possible combinations of the five parameters ($2^5 - 1$, here "2" indicated whether a specific parameter changes across conditions, and "−1" indicated that the null model was excluded). The Bayesian estimation for each candidate model was performed with MatBugs (https://github.com/matbugs), a software package that uses Markov chain Monte Carlo (MCMC) simulation to obtain the posterior distributions of the model parameters and the model's best-fitting parameters (Donkin, Averell, Brown, & Heathcote, 2009). To determine the best model, we used each model's best-fitting parameters to calculate the deviance information criterion (DIC). The DIC is a hierarchical modeling generalization of the Bayesian information criterion (BIC) and is frequently used in the Bayesian model selection process where the

posterior distributions are estimated by MCMC simulation. The model with the minimal summed DIC across participants was suggested to have the best description of the data. We also performed Wilcoxon sign tests between all pairs of the models to validate the choice of the best model.

The outputs of the LBA model were the mean estimates of the five model parameters across trials. Then, we used maximum likelihood estimation (see Equation S1 in Supplementary Text S1) to obtain the single trial estimates of the drift rate $\hat{v}$ and start point $\hat{a}$ (van Maanen et al., 2011). The single trial decision caution was defined as the difference between the mean estimates of the response threshold b and the single trial start point $\hat{a}$.

fMRI data preprocessing

MRI data were separately preprocessed in Brain Voyager QX (Brain Innovations) and SPM12 (www.fil.ion.ucl.ac.uk/spm) following similar procedures. The preprocessed data in Brain Voyager QX was used to define the regions of interest (ROIs) and perform ROI-based analyses. The preprocessed data in SPM12 was used for the single trial analysis and the dynamic causal modelling (DCM). In both procedures, the first four volumes of each functional run were discarded, allowing longitudinal magnetization to reach a steady state. In Brain Voyager QX, the anatomical data from different sessions were aligned with each other and then transformed into Talairach coordinate space. The anatomical data were also used for 3D cortex reconstruction and inflation. The preprocessing of functional data included slice timing correction, head movement correction, temporal high pass filtering (three cycles), and removal of linear trends and spatial smoothing (Gaussian filter; full width at half-maximum, 8 mm). In SPM12, all fMRI images were realigned to the first volume of the first run of the first session and corrected for acquisition delay, with the middle slice serving as the reference. The images were then normalized to the MNI coordinate space using an EPI template. The normalized images were smoothed with a Gaussian kernel with 8 mm FWHM.

Single-trial analysis of fMRI data with ICA

Single trial hemodynamic response (HR) amplitudes were estimated with the methods proposed in Eichele et al. (2008). To increase the statistical power of the analysis and to isolate the components that maximally represent the decision-related information in fMRI signal, we applied the group spatial independent component analysis (ICA, Calhoun, Adali, Pearlson, & Pekar, 2001) on the preprocessed fMRI data from the pretest session using GIFT (http://icatb.sourceforge.net). The number of the components was set to 30. The group spatial ICA was implemented by infomax algorithm (Bell & Sejnowski, 1995; Correa, Adali, & Calhoun, 2007). To assess the reliability of the estimated independent components (ICs), we repeated the decomposition process 100 times with random initial conditions and bootstrapped based on the ICASSO approach (Himberg, Hyvärinen, & Esposito, 2004; Himberg & Hyvärinen, 2003). Individual ICs with a robustness index lower than 0.9 or associated with artifacts representing signals from large vessels, ventricles, and motion were excluded from further analyses, leaving 20 ICs for further analyses. The time courses of the remained ICs were then filtered with a 72-s high pass fifth-order Butterworth digital filter and then normalized to unit variance.

For each participant, each run, and each component, the event-related hemodynamic response function (HRF) for the selected ICs was de-convolved by forming the convolution matrix of all trial onsets with an assumed kernel length of 20 s and then multiplying the Moore-Penrose pseudoinverse of this matrix with the filtered and normalized IC time course. The estimated HRFs convolved with the stimuli matrix, which contained separate predictors for each trial onset, to obtain the design matrix. The single trial HR amplitudes were recovered based on the design matrix and the normalized IC time course, using linear regression model.

ROI definition

Retinotopic visual areas (V1, V2, and V3) were defined by a standard phase encoded method (Engel, Glover, & Wandell, 1997; Sereno et al., 1995). During the scanning, the participants maintained fixation while viewing a rotating wedge. The boundaries between visual areas were delineated using field-sign mapping. The motion-responsive voxels (V3A, MT+) were identified with a localizer procedure (Huk, Dougherty, & Heeger, 2002). We presented random dot stereograms, which were static for 24 s and then traveled toward and away from the fixation for 8 s. The moving/stationary cycle repeated nine times. The size of the stimulus aperture was the same as that used in the main experiment. A general linear model (GLM) was then used to extract the ROIs.

Percentage signal change analysis

The percentage signal changes of the event-related BOLD signals were calculated separately for each subject, following the method used by Kourtzi and Kanwisher (2000). Specifically, in each run we

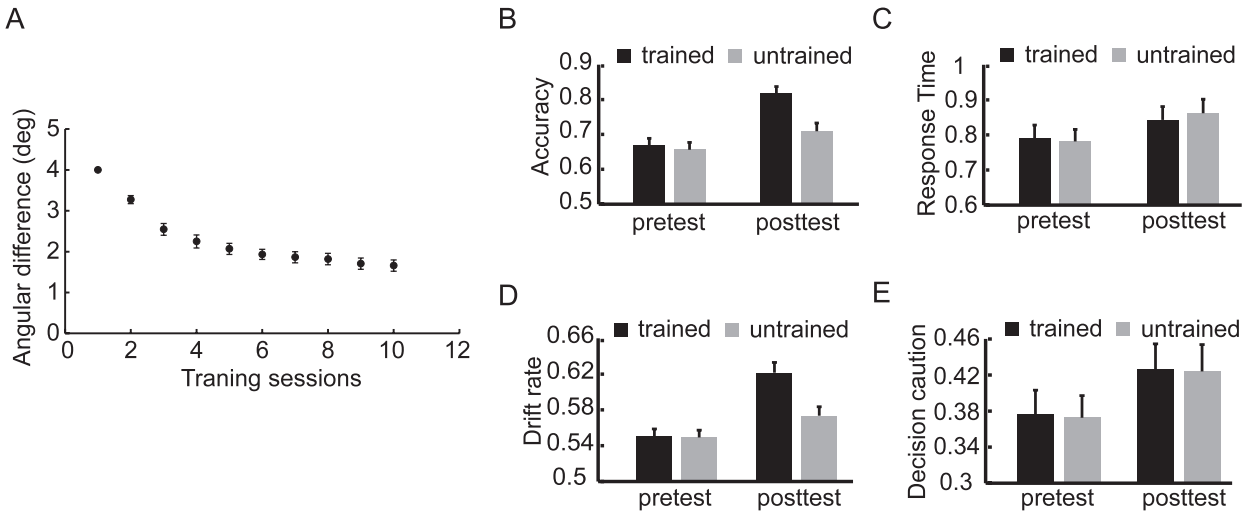

Figure 2. Behavioral and modeling results. (A) Behavioral performance in the training sessions. (B) Accuracy in the pretest and posttest sessions. (C) Response times in the pretest and posttest sessions. (D) Estimated drift rate in the pretest and posttest sessions. (E) Estimated decision caution in the pretest and posttest sessions. Error bars represent standard errors.

extracted the fMRI signal intensity for each trial type at each of the 12 corresponding time points starting from 4 TRs before the stimulus onset and ending at the 8th TR after the stimulus onset. The time courses of each condition were averaged across all the voxels within the predefined ROI and across all trials. The averaged event-related time courses were then converted to the time courses of percentage signal change for each type of trials by subtracting and then dividing by the mean time course of the fixation trials. The time courses of percentage signal change was then averaged across all runs and the peaks of the time course were used to investigate the effect of perceptual learning.

Results

Behavioral learning effect

Participants' behavioral performance enhanced substantially over the course of training (Figure 2A). The angular difference in the last training session (mean = 1.66°, $SEM = 0.14°$) was significantly reduced in comparison to the angular difference in the first training session, 4°, paired $t(21) = -17.07$, $p < 0.001$. The improved discriminability was confirmed by analyzing the mean discrimination accuracy and RT obtained in the pretest and posttest fMRI sessions. A repeated measures ANOVA on discrimination accuracy, motion direction (trained vs. untrained) × session (pretest vs. posttest; Figure 2B) revealed significant effects of motion direction, $F(1, 21) = 14.64$, $p = 0.001$, $\eta_p^2 = 0.411$; session, $F(1, 21) = 33.78$, $p < 0.001$, $\eta_p^2 = 0.617$, and their interaction, $F(1, 21) = 13.87$, $p = 0.001$, $\eta_p^2 = 0.398$. Further tests of simple main effects revealed that the accuracy for the trained direction was significantly higher than the untrained direction in the posttest session, $F(1, 21) = 21.30$, $p < 0.001$, whereas no significant difference was observed before the training, $F(1, 21) = 0.55$, $p = 0.47$. A repeated measures ANOVA also showed that the RTs in the posttest session were marginally slower than those in the pretest session, $F(1, 21) = 4.28$, $p = 0.051$, $\eta_p^2 = 0.284$ (Figure 2C). Neither a significant effect of motion direction, $F(1, 21) = 0.66$, $p = 0.42$, nor an interaction between motion direction and session, $F(1, 21) = 2.20$, $p = 0.15$, was observed.

Learning effect on fitted model parameters

We fitted thirty-one variants of the LBA model to the behavioral data from the pretest and posttest fMRI sessions (see Materials and methods for constraints on different model variants). The best model (the one with the lowest DIC value across participants) allows the parameters *a, b, v,* and *s* to vary across conditions while t_0 remains fixed (see Supplementary Figure S2 for the fitting results of the best model). Wilcoxon sign tests of the DIC value revealed that this best model was significantly superior to the other twenty-four models ($p < 0.01$, FDR corrected). The remaining six models were defined as suboptimal models. We repeated all analyses based on the parameters from these suboptimal models, and similar results were revealed. Therefore, we focused on the best model with the minimum DIC value.

Learning effects on drift rate

We examined the effect of training on the model parameters. For the drift rate v (Figure 2D, see Supplementary Figure S3 for results of decision boundary, start point, and deviation of the drift rate), a repeated measures ANOVA (motion direction × session) revealed significant effects of motion direction, $F(1, 21) = 15.60$, $p = 0.001$, $\eta_p^2 = 0.426$; session, $F(1, 21) = 48.27$, $p < 0.001$, $\eta_p^2 = 0.697$; and their interaction, $F(1, 21) = 25.43$, $p < 0.001$, $\eta_p^2 = 0.548$. The drift rate for the trained direction was significantly higher than the untrained direction in the posttest session, $F(1, 21) = 27.22$, $p < 0.001$, while no significant difference was observed before the training, $F(1, 21) = 0.08$, $p = 0.78$.

Next, we examined whether the observed behavioral learning effect can be accounted by the change of the drift rate (C. C. Liu & Watanabe, 2012; Petrov et al., 2011). We defined a learning modulation index (LMI, Jehee et al., 2012) [(posttest − pretest along the trained direction) − (posttest − pretest along the untrained direction)] and calculated the LMIs for both the behavioral accuracy and model parameters (drift rate v, response threshold b, and decision caution $b - a/2$). We then performed a regression analysis based on the calculated LMIs and the results showed that only the LMI of the drift rate can account for the variance of the behavioral LMI across participants: regression, $F(3, 12) = 15.48$, $p < 0.001$, adjust $R^2 = 0.67$; $\beta = 0.73$, $p < 0.001$, not that of the decision caution, $\beta = 0.214$, $p = 0.26$, nor the response threshold, $\beta = -0.01$, $p = 0.97$.

Session effect on decision caution

Furthermore, we observed a significant session effect on the decision caution, $F(1, 21) = 8.45$, $p < 0.01$, $\eta_p^2 = 0.287$ (Figure 2E). We defined a session index (SI = posttest − pretest) for both RT and decision caution. The SI of the decision caution was strongly correlated with the SI of RT across participants (correlation efficient = 0.97, $p < 0.001$), suggesting that the slowed RT after the training was associated with the higher decision caution during the posttest session.

These modeling results suggest that the behavioral learning effect can be well explained by the improvement of sensory information accumulation. However, perceptual decision-making is a complex process that involves multiple cognitive components and brain regions (Gold & Shadlen, 2007; Heekeren et al., 2008). Specifically, the process of sensory information accumulation is modulated by both bottom-up sensory input (Shadlen & Newsome, 2001) and top-down attentional feedback (Kelly & O'Connell, 2013; Krajbich, Armel, & Rangel, 2010). To elucidate the neural mechanism underlying the learning-specific improvement, we first identified the decision-related network based on fMRI signal and then determined the functional roles of the network's components in perceptual learning.

Brain network for sensory information accumulation

The behavioral and modeling results showed that the learning effect could be explained by the increase of drift rate. To unravel the neural mechanisms underlying the perceptual learning, the neural correlates of the drift rate need to be identified. Specifically, we decomposed the fMRI data obtained in the pretest session into spatial ICs. Each IC represented an independent source of signal and the fMRI time courses were the weighted sum of all ICs' time courses. We decomposed the ICs solely based on the fMRI data from the pretest session to ensure that the ICs were related to the decision process and the subsequent analyses on the ICs were not biased by the learning process. For each IC, the algorithm assigned a weight for each voxel. IC's spatial map was defined as the 150 voxels with the largest weights. We de-convolved each IC's time course to estimate the HRF and extracted the single trial HR amplitudes with a linear regression model. We then calculated the partial correlations between the estimated single trial drift rates and the single trial HR amplitudes of all ICs , controlling for the effects of the stimulus duration and the motion direction (Ho, Brown, & Serences, 2009; van Maanen et al., 2011; Zhang, Hughes, & Rowe, 2012). We examined the representation of drift rate in each IC by comparing the obtained partial correlation coefficients across participants with zero (FDR corrected for 20 ICs). The results showed significant effects for the ICs located at ventral premotor cortex, PMv, $t(21) = 2.769$, $p < 0.05$, FDR corrected; and supplementary eye field, SEF, $t(21) = 2.697$, $p < 0.05$, FDR corrected; as well as a trend of significance at the frontoparietal network, FPN, $t(21) = 2.192$, $p = 0.09$, FDR corrected, that included frontal eye field (FEF) and intraparietal cortex (IPS). We refer the areas where the drift rate-correlated ICs (PMv, SEF, and FPN) located as the decision network of the motion direction discrimination task in the present study (Figure 3A).

Learning effects within decision network

Given the significant learning effect on the drift rate, we expected similar learning effects in the decision network that correlated with drift rates. We examined learning-specific signal changes within the identified decision network and two motion selective areas (V3A and MT+), as well as the between-region connectivity. Specifically, for PMv and SEF, we

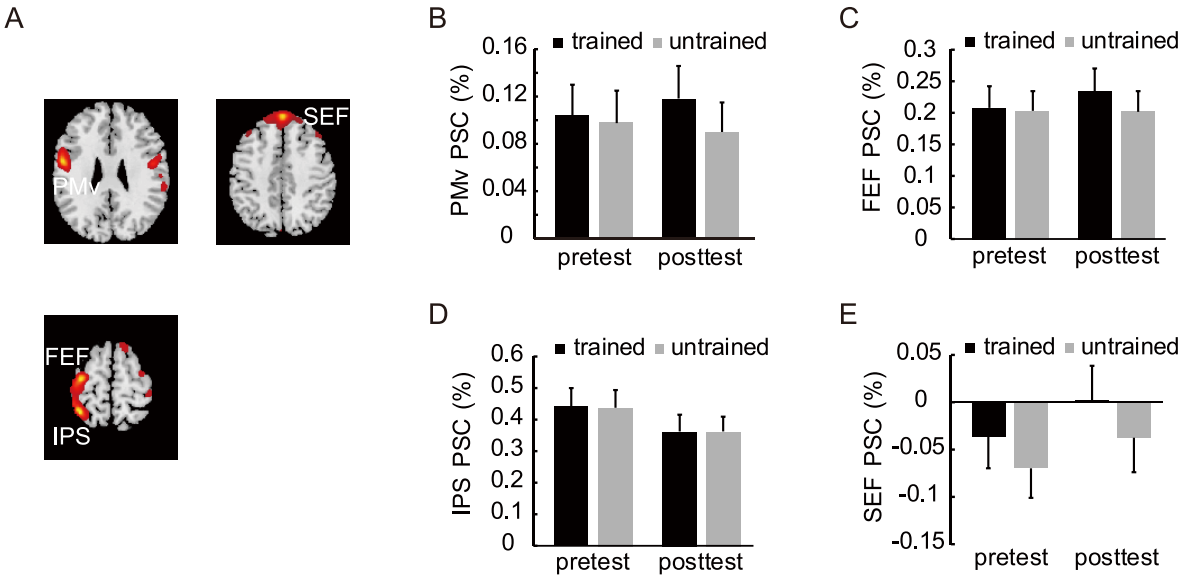

Figure 3. Drift rate-correlated independent components and the percentage signal changes of the fMRI signals in these areas. (A) The spatial map of the three drift rate-correlated ICs (transversal view): ventral premotor cortex (PMv), supplementary eye field (SEF), and the fronto-parietal network (FPN) that included frontal eye field (FEF) and intraparietal cortex (IPS). (B–E) Percentage signal changes of the fMRI signals from these brain areas. Error bars represent standard errors.

selected 150 voxels with the largest weights based on the spatial map of the ICA analysis. For FPN (including FEF and IPS), we chose a voxel with the largest weight based on the spatial map of the FPN network for each area, and then defined a spherical ROI (8 mm radius, ~60 voxels) centering at this voxel. The following analyses were performed on the voxels' signals after preprocessing rather than those of the IC time courses. There were two considerations for the choice of the signal. First, the IC time courses were decomposed based on the fMRI data from the pretest session, making them unavailable for calculating the cross-session learning effects. Second, although both FEF and IPS were within the IC of FPN, and they share the same IC time course, they may contribute differently to the observed learning effect. Analyzing the voxel signals from the two regions can solve this problem.

Learning effects on percent signal changes

To compare our results with the previous study (Chen et al., 2015), we calculated the LMI using the percent signal changes for all ROIs. One sample t tests revealed direction-specific signal enhancements in PMv, $t(21) = 2.15$, $p = 0.032$, one-tailed, FDR corrected; and FEF, $t(21) = 2.21$, $p = 0.032$, one-tailed, FDR corrected; as well as a signal reduction in V3A, $t(21) = -3.00$, $p = 0.003$, one-tailed, FDR corrected; and MT+ $t(21) = -5.03$, $p < 0.001$, one-tailed, FDR corrected.

For both PMv and FEF (Figure 3B and 3C), the repeated measures ANOVAs (motion direction × session) on the percentage signal change showed significant effects of motion direction, PMv: $F(1, 21) = 5.78$, $p = 0.025$, $\eta_p^2 = 0.216$; FEF: $F(1, 21) = 4.72$, $p = 0.04$, $\eta_p^2 = 0.184$; and two-factor interactions, PMv: $F(1, 21) = 4.63$, $p = 0.043$, $\eta_p^2 = 0.181$; $F(1, 21) = 4.89$, $p = 0.038$, $\eta_p^2 = 0.189$. There were no significant effects of session; PMv: $F(1, 21) = 0.046$, $p = 0.83$; FEF: $F(1, 21) = 0.311$, $p = 0.58$. Further simple effect analyses revealed significantly higher response for the trained than for the untrained direction in the posttest session, PMv: $F(1, 21) = 7.656$, $p = 0.012$; FEF: $F(1, 21) = 11.58$, $p = 0.003$, whereas no significant differences were observed before training, PMv: $F(1, 21) = 0.59$, $p = 0.45$; FEF: $F(1, 21) = 0.159$, $p = 0.69$. In addition, the same repeated measures ANOVA on IPS (Figure 3D) showed a significant signal reduction that was not specific to the trained direction: session, $F(1, 21) = 7.795$, $p = 0.011$, $\eta_p^2 = 0.271$; motion direction, $F(1, 21) = 0.023$, $p = 0.88$; interaction, $F(1, 21) = 0.117$, $p = 0.74$. No learning-related changes were found in SEF (Figure 3E).

For both V3A and MT+ (Figure 4), the repeated measures ANOVAs (motion direction × session) revealed significant interaction effects, V3A: $F(1, 21) = 8.979$, $p = 0.007$, $\eta_p^2 = 0.3$; MT+: $F(1, 21) = 25.301$, $p < 0.001$, $\eta_p^2 = 0.546$. Further simple effect analyses showed significant response reductions in post- than pretest session for the trained direction, V3A: $F(1, 21) = 7.867$, $p = 0.011$; MT+: $F(1, 21) = 6.30$, $p = 0.02$. Such effect was not observed for the untrained direction, V3A: $F(1, 21) = 1.56$, $p = 0.23$; MT+: $F(1, 21) = 0.002$, $p = 0.97$. None of the other effects were significant ($p > 0.05$ for

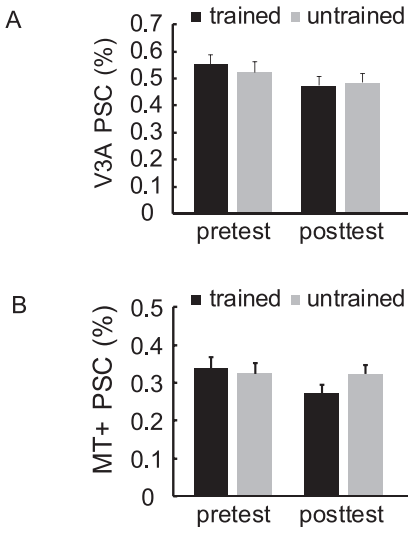

Figure 4. Percentage signal changes of the fMRI signals from the motion selective sensory areas (V3A and MT+). Error bars represent standard errors.

all comparisons), except for a main effect of motion direction in MT+, $F(1, 21) = 9.652$, $p = 0.005$, $\eta_p^2 = 0.315$.

Learning modulates feedforward connectivity

Finally, we selected the brain areas with significant learning effects (V3A, MT+, PMv, IPS, and FEF) and constructed DCM models with SPM12 to examine whether learning altered the connectivity among them. The models were based on the voxels' signals after preprocessing and consisted of bidirectional connections between any two out of the five areas. The network received external stimulus inputs (motion stimuli) from both V3A and MT+ (Chen et al., 2015), with the motion direction (trained vs. untrained) serving as a modulator. We tested nine candidate models with the assumption that training had influenced different connections in each model (Table 1). From Model 1 through Model 4, we assumed feedforward or feedback connection between the sensory areas (V3A or MT+) and decision-related areas (IPS, FEF, and PMv). From Model 5 through Model 7, we assumed connections between the areas within the decision network. In Models 8 and 9, we also considered the connections between two areas within a single IC (i.e., FPN).

	Direction of model connections	
Model ID	From	To
1	V3A	IPS, FEF, PMv
2	IPS, FEF, PMv	V3A
3	MT+	IPS, FEF, PMv
4	IPS, FEF, PMv	MT+
5	PMv	IPS,FEF
6	IPS,FEF	PMv
7	IPS	FEF
	FEF	IPS
8	IPS	FEF
	V3A	PMv
9	FEF	IPS
	PMv	V3A

Table 1. DCM model definitions.

Bayesian model selection with a random effect analysis (Stephan, Penny, Daunizeau, Moran, & Friston, 2009) revealed strong evidence in favor of Model 8 (Figure 5A and 5B) that assumed modulation of learning on the feedforward connections from V3A to PMv and from IPS to FEF. The coefficients of the modulation effect in Model 8 were evaluated with paired t tests and the results showed a strengthened connection from V3A to PMv, $t(21) = 2.33$, $p = 0.03$ (Figure 5C), and from IPS to FEF, $t(21) = 2.72$, $p = 0.01$ (Figure 5D). Furthermore, one sample t tests showed that neither the connection from V3A to PMv, $t(21) = -0.964$, $p = 0.35$, nor the connection from IPS to FEF, $t(21) = -1.733$, $p = 0.1$, showed significant difference between the trained and untrained directions in the pretest session, indicating that the observed modulation was due to the enhanced training effects.

Discussion

In the current study, we trained participants with a motion direction discrimination task. The results showed a behavioral improvement that was largely specific to the trained direction (Ball & Sekuler, 1987) and was accompanied by the increased drift rate of information accumulation (Dutilh et al., 2009; C. C. Liu & Watanabe, 2012; Petrov et al., 2011; Zhang & Rowe, 2014). Decomposing fMRI signal into independence components revealed a set of decision-related components that covaried with the drift rate on a trial-by-trial basis. Further analyses based on the fMRI signals in the areas corresponding to these decision-related components and the motion responsive sensory areas suggest that perceptual learning facilitates information accumulation at different levels of processing. There are three main findings from the present study.

First, the behavioral improvement was accompanied by a signal reduction in V3A, and MT+ specific to the trained direction. The two areas are essential for motion perception (Mckeefry, Burton, Vakrou, Barrett, & Morland, 2008; Salzman, Murasugi, Britten, & Newsome, 1992; Tootell et al., 1997) and motion perceptual learning (Chen et al., 2015; Shibata et al.,

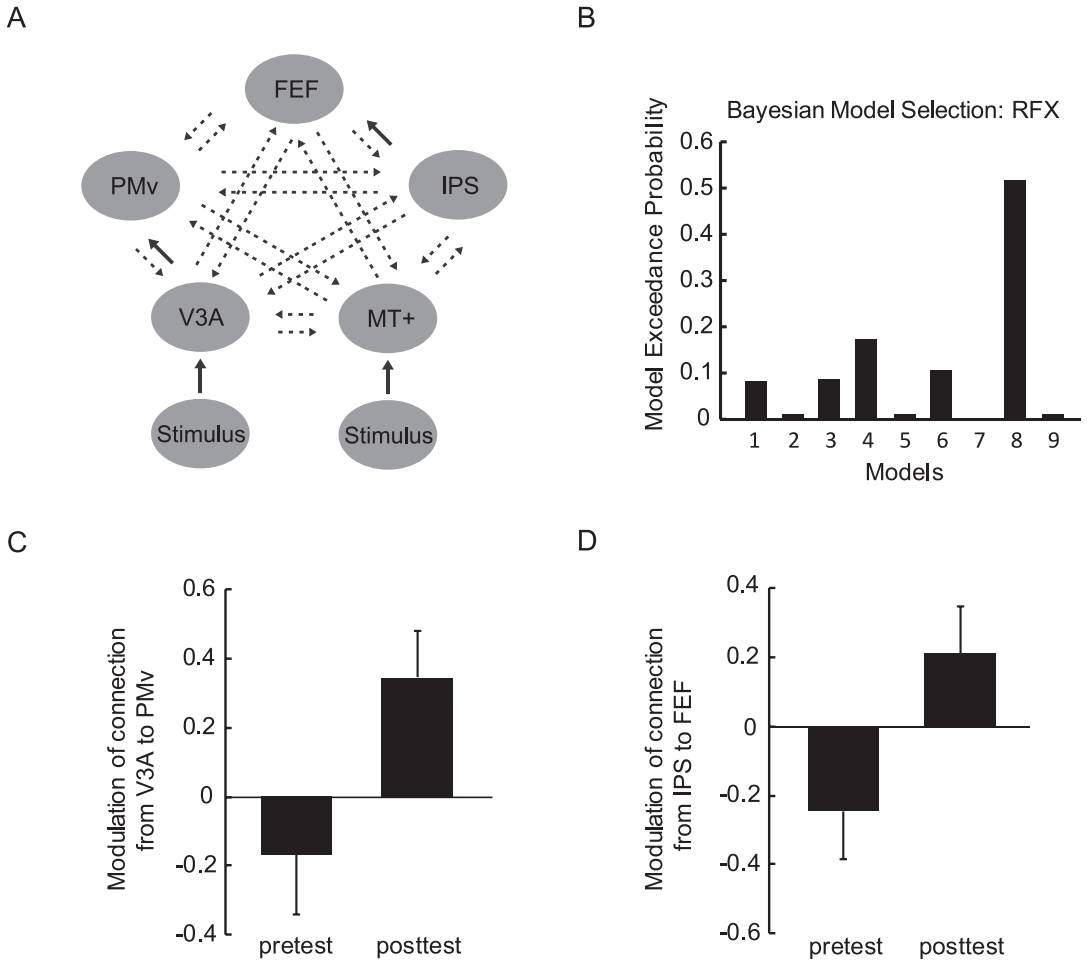

Figure 5. DCM results. (A) The optimal model (Model 8) after the model selection. The dash arrows represent the intrinsic connections between brain areas. The solid arrows represent the modulation of training on the connections on top of the intrinsic connections. (B) Exceedance probability in a random effect analysis. The Bayesian model selection showed that Model 8 was the optimal model. (C) Modulation effect of training on the connection from V3A to PMv. (D) Modulation effect of training on the connection from IPS to FEF. Error bars represent standard errors.

2012). The decreased brain activity after training could be explained by the sharpened tuning of neuronal representations (Mukai et al., 2007) or the modified excitation-inhibition interaction in sensory cortex (Schoups et al., 2001; Teich & Qian, 2003). Importantly, this reduction in V3A and MT+ could serve as another supporting evidence for the sensory modification hypothesis. Meanwhile, a nonspecific reduction of activity in IPS was observed. This deactivation in IPS could be interpreted by the learning-elicited automaticity that attentional resource is less required when a task is repeated for many times (Bays, Visscher, Le Dantec, & Seitz, 2015; Mukai et al., 2007). It is worth noting that IPS is a multifunction cortical region and its activity may consist of both attentional and decisional signals. In the present study, the overall signal of the defined IPS area was likely to be dominated by the attentional process, and the rest of its signal was related to the decision process and was captured by the ICA analysis. However, quantitative measurement of the contributions of different processes to the fMRI activity in IPS is beyond the scope of the present study. Future experiments can be designed to specifically examine this issue.

Second, a training-specific signal enhancement was observed in PMv and FEF, which were identified through the correlational analysis with the drift rate. Previous physiological studies have suggested that PMv (Romo, Hernandez, & Zainos, 2004) and FEF (Kim & Shadlen, 1999) are the critical regions for perceptual decision making in the monkey's brain. Meanwhile, fMRI studies with human subjects also demonstrated the similar decision networks of brain areas as in our results of the correlational analysis (Kayser, Buchsbaum, Erickson, & Esposito, 2010; T. Liu & Pleskac, 2011). Importantly, in consistent with the observed learning effects on LIP activity in a neurophysiological study (Law & Gold, 2008), we observed direction

specific learning effects in multiple cortical sites of the decision making network, indicating the involvement of the decision network in the build-up of the perceptual learning effects. The enhanced signals in PMv and FEF mirrored the signal reduction in V3A and MT+, suggesting the co-occurrence of the refined processing in sensory and decision areas as the product of perceptual learning.

Third, the DCM results revealed that the effective connectivity from V3A to PMv and from IPS to FEF was enhanced after training. The increased feedforward connection from V3A to PMv can be well explained by the improved sensory accumulation process due to perceptual training (Dosher et al., 2013; Dosher & Lu, 1998; Petrov et al., 2005). However, the enhanced connectivity from IPS to FEF within the fronto-parietal network needs to be explained with caution. One possible interpretation could be that, perceptual training refined the processing within the decision network, including the communications between the decision areas. However, this hypothesis needs to be carefully examined with future experiments. Also, due to the temporal limitation of the DCM approach on fMRI signal, future investigations with electrophysiological measurements are required for fully understanding the between region modulatory effect.

A number of studies have investigated the neural mechanism of motion perceptual learning in human brain (Chen et al., 2015; Shibata et al., 2012; Shibata, Sasaki, Kawato, & Watanabe, 2016). Related to the present study, Chen et al. (2015) also revealed negative LMI learning effect in V3A and a similar trend in MT+. The two studies agree with each other in that motion direction discrimination training induces BOLD signal reduction in motion selective sensory areas that is largely specific to the trained direction. Further, investigations with MVPA approach have indicated that the activity patterns in V3A rather than MT+ robustly encode the learning-induced selectivity enhancement (Chen et al., 2015; Shibata et al., 2012, Shibata et al., 2016). Although we could not perform a proper MVPA analysis due to the limitation of the event-related design, our DCM results suggest strengthened feedforward connection from V3A to PMv, but not from MT+ to higher areas, in line with the critical role of V3A in refining sensory representation in motion perceptual learning. These results are supportive of the feature-based learning (Shibata et al., 2014; Watanabe & Sasaki, 2015).

Despite the consistent findings of strengthened feedforward connections from V3A to higher-level decision-related areas, the present study differed from Chen et al. (2015) in the identified high level areas that connected to V3A (i.e., PMv vs. IPS). This discrepancy may be attributed to the methods of IPS definition (motion responsive voxels in Chen's study vs. drift rate correlated ICs), or the experimental design adopted during the fMRI session (block vs. event-related design). Nevertheless, both studies consistently showed enhanced feedforward connections from V3A to higher cortical areas that may be interpreted as an optimization of the connections between sensory and decision-making areas. In addition, we also identified strengthened feedforward connection from IPS to FEF and positive LMI effects in PMv and FEF, which extended previous studies. The opposite LMI effects between the sensory areas (V3A and MT+) and decision-related areas (PMv and FEF) suggest that learning may act differently in the lower and higher areas. Previous investigation on perceptual decision has shown that the higher activation in frontal decision-related areas is associated with better sensory evidence (Heekeren, Marrett, Bandettini, & Ungerleider, 2004). The positive LMI effects in PMv and FEF agree with this proposal. Importantly, the strengthened feedforward connections and the positive LMI effects in the decision-related areas could be the evidence for the enhanced sensory information read-out during the decision process, reflecting the task-based component in perceptual learning (Shibata et al., 2014; Watanabe & Sasaki, 2015). These results are also consistent with the Maniglia-Seitz model that perceptual learning effect is jointly determined by multiple brain systems (Maniglia & Seitz, 2018).

The finding of general increase in RTs after training is likely due to an increase of decision caution, as indicated by LBA model fitting. We believe that the more cautious response could be induced by our training paradigm. In the training phase, the task difficulty increased over sessions and may compel participants to make more cautious decision in the posttest session. An alternative interpretation of the slowed RT is due to the state of learning at the end of training as the procedure may lead to an emphasis on evidence that would not be the same as the best evidence in the posttest session. However, this interpretation may be less plausible for two reasons. First, if the evidence used by participants in the posttest session was not the optimal, the RT along the untrained direction should not change from the pretest session. This was not the case as we observed an increase on RT for both the trained and untrained directions. Second, the drift rate and accuracy should decrease in the posttest session for the trained direction if nonoptimal evidence was used for decision, which contradicts with the present behavioral results.

The LBA model used in the current study is a simplified version of a family of sequential sampling models that simulates the perceptual decision process. The simplicity of the LBA model enables posterior parameter estimations on a trial-by-trial basis, making the model an ideal candidate for correlating the

fluctuation of the decision process with collected brain imaging signals (Brown & Heathcote, 2008; Donkin et al., 2011; Ho et al., 2009; van Maanen et al., 2011; Zhang et al., 2012). It is noteworthy that many psychological models of decision-making have been proposed, and they all share a similar accumulation-to-threshold framework (Bogacz et al., 2006; Smith & Ratcliff, 2004; Zhang, 2012). Recent studies showed improvement in sensory information accumulation after training by using the drift-diffusion model (Dutilh et al., 2009; C. C. Liu & Watanabe, 2012; Petrov et al., 2011; Zhang & Rowe, 2014), which is consistent with our results from the LBA model. However, the diffusion model explicitly includes within-trial variability, making it difficult to estimate the single-trial drift rate (Ratcliff & McKoon, 2008). Nevertheless, our results are unlikely to depend on the particular model we used, as the LBA model reserves high correlations on the estimated parameters compared with the drift diffusion model (Donkin et al., 2011). To further validate this idea with our data, we estimated the parameters with the classical drift diffusion model. The drift rate estimated with drift diffusion model revealed a similar pattern of learning effect. More importantly, the drift rate estimated from two models were highly correlated ($r > 0.762$ for all four conditions, $p < 0.001$ for all four conditions; see Supplementary Figure S4) across participants.

One possible concern about our finding is that behavioral accuracy and estimated drift rate showed similar patterns of results, and the changes of fMRI activity could reflect the changes in performance level. We suggest that these two indices reflect the behavioral performance at different levels. For the motion discrimination task, accuracy reflects the final output of the discrimination process. However, without the decomposition of this process with the LBA model, we would not be able to weight the contributions of different components (drift rate, boundary separation, nondecision time, etc.) to the changes in directly measurable behavioral performance (i.e., accuracy and response time). For example, training could enlarge the boundary separation while leaving drift rate unchanged or increase drift rate while leaving boundary separation constant. In both cases, we could observe increased accuracy. As the aim of the present study was to identify the decision network involved in the discrimination task and to investigate the learning effect within the network, drift rate can serve as a better index to capture the trial-by-trial fluctuation in the decision process, whereas accuracy is calculated based on the whole set of behavioral data and does not have such advantage.

There is an alternative approach in designing a learning experiment by adopting different tasks in training and tests, so that the task performance could remain constant before and after training (Furmanski, Schluppeck, & Engel, 2004). In the present study, we used the discrimination task throughout the experiment for two reasons. First, the aim of the present study was to identify the decision network involved in the discrimination task and to investigate the learning effect within the network. It was necessary to use the same angle difference for the trained and untrained directions both before and after training, making sure that training was the only difference across conditions. If we changed the angle difference to control for the task performance, the drift rate may be the same across different experimental conditions, and we would miss the learning effect in the decision network. We agree that with this design the task difficulty might differ across conditions, which however, might not contribute largely to our main effects, as indicated by a recent study demonstrating little impact of task difficulty on the activity in V3A and MT+ using similar stimuli and task design (Na et al., 2018). More importantly, if changes in task difficulty after training could contribute to the neural activity in the frontal areas, we would expect reduced signals with easier task. This is in contrast to our findings in IPS, PMv, and FEF. Further, in a closely compared study in the manuscript, Chen et al. (2015) measured participants' discrimination threshold before each fMRI session and used this threshold in the scanner to make sure that the task performance of every condition is around 79.4%. With this design, similar training effects were observed in MT+, V3A, and IPS as in the present study. Therefore, it is unlikely that our results were due to the changes in performance level of the discrimination task. Second, it has been suggested that the transfer of learning between high signal-to-noise stimuli in discrimination task and low signal-to-noise stimuli in detection task is asymmetrical in a variety of perceptual learning tasks (Chang, Kourtzi, & Welchman, 2013; Dosher & Lu, 2005; F. Yang, Wu, & Li, 2014). These results suggest that detection task and discrimination task may not share the same mechanisms (Hol & Treue, 2001). Furthermore, we would like to emphasize that the improvement in performance level (i.e., accuracy) was the main behavioral results of learning. Therefore, the learning-induced changes of BOLD activity should co-occur with the improvement in performance level of the task. Beyond the results in performance level, we decomposed the decision process with the LBA model, and therefore were able to suggest which variables (drift rate, boundary separation, nondecision time, etc.) actually contributed to the observed behavioral effect. However, we believe that this issue deserves future investigations.

There is another issue in the present study that deserves particular explanation. In our fMRI sessions, the stimulus presentation terminated when the partic-

ipant made a response. We had this design to ensure that the fMRI signal related to information accumulation was not affected by losing sensory input (e.g., fixed shorter duration) or adding extra sensory input after decision process (e.g., fixed longer duration). One could argue that, because fMRI signal may be correlated with the length of stimulus duration, it was possible that the observed learning effects in fMRI signal were due to the variations in stimulus duration. However, our main results are unlikely to be confounded by this factor for two reasons. First, we observed training-specific signal reduction in motion responsive sensory areas (V3A and MT+). As the RT (and hence the stimulus duration) was longer after training and there was no significant difference between the trained and untrained directions, the fMRI signals in the sensory areas could not be explained by the stimuli duration. Therefore, the fMRI signals in the higher areas were even less likely to reflect the stimulus duration. In fact, the significant interactions in PMv and FEF could not be explained by the main effect of RT, and the activation in IPS was even reduced in the posttest session where the RTs were increased. Second, the single trial correlation analysis revealed positive correlations between the three ICs and drift rate. If our results were caused by stimulus duration, negative correlation should be expected.

Finally, training-induced perceptual and decisional biases could also contribute to the observed learning effect. It has been suggested that the tasks that begin with a fixed line reference and followed by a very long stimulus duration are particularly susceptible to decision- (Jazayeri & Movshon, 2007; Zamboni, Ledgeway, McGraw, & Schluppeck, 2016) and adaptation-induced biases. First, our experimental design of the discrimination task precludes the possibility that the perceived angle of the discrimination boundary could be changed by training. In the experiment, the fixed line reference appeared at the beginning of each trial for 500 ms, and followed by a 500–1,000 ms blank interval, after which the motion stimulus was shown. The direction of the motion stimuli can either be clockwise or counterclockwise relative to the reference, making the perceive angle of the discrimination boundary unlikely to be biased towards one of the directions. Second, we only asked the participants to perform the fine discrimination task in the present study, rather than the estimation task used in Jazayeri's study. It has been suggested that there was no systematic bias in behavioral choices for the fine discrimination performance, whereas the subjects' estimates were biased when they were asked to perform the estimation task (Jazayeri & Movshon, 2007). Therefore, it was unlikely that our results can be attributed to the decision bias. Third, the perceived angle of the motion stimuli after training could be biased. Previous studies have investigated the training effect on the reference repulsion (Szpiro, Spering, & Carrasco, 2014) and the motion repulsion (Jia & Li, 2017). Importantly, based on the recurrent model of the discrimination learning (Teich & Qian, 2003), training would decrease the activity of neural population preferring the trained direction, which is also consistent with the reduced LMI in V3A and MT+ in the current study. According to the model, this reduction would change the perceived direction of the motion stimuli (moves several degrees away from the trained direction) and repel it further away from the trained direction (i.e., perceptual bias). This repulsive effect would further enhance participants' discrimination sensitivity. In this framework, the perceptual bias and the enhanced sensitivity could be attributed to the same neural mechanism, which is also the source of the increased drift rate after training. Fourth, it has also been shown that motion adaptation and perceptual learning interact with each other (McGovern, Roach, & Webb, 2012). However, the stimulus duration in the present study was the same as the subject's RTs (around 800 ms on average). This stimulus duration is much shorter than that is usually used in the adaptation studies (more than 20 s for initial adapt and few seconds for each top-up). Therefore, it was unlikely that our results were due to a strong adaptation effect as demonstrated literature. Nevertheless, perceptual bias plays important roles in almost all perceptual tasks. We could not completely rule out its contribution to perceptual learning effect. Future investigations with specific designs are required to address this issue.

Keywords: LBA, drift rate, fMRI, motion

Acknowledgments

We thank Zili Liu for helpful comments and suggestions on this article. This work was supported by grants to S.L. from National Key R&D Program of China (2017YFB1002503) and the National Natural Science Foundation of China (31470974, 31230029, 31271081) and to J.Z. from European Research Council Starting Grant (716321). The scanning facilities was supported by the Ministry of Science and Technology of China (2005CB522800), National Natural Science Foundation of China (30621004, 90820307), and the Knowledge Innovation Program of the Chinese Academy of Sciences.

Commercial relationships: none.
Corresponding author: Sheng Li.
Email: sli@pku.edu.cn.
Address: School of Psychological and Cognitive Sciences, Peking University, Haidian, Beijing, China.

References

Adab, H. Z., & Vogels, R. (2011). Practicing coarse orientation discrimination improves orientation signals in macaque cortical area V4. *Current Biology*, *21*, 1661–1666, https://doi.org/10.1016/j.cub.2011.08.037.

Ahissar, M., & Hochstein, S. (1997, May 22). Task difficulty and the specificity of perceptual learning. *Nature*, *387*(6631), 401–406.

Ball, K., & Sekuler, R. (1987). Direction-specific improvement in motion discrimination. *Vision Research*, *27*, 953–965.

Bays, B. C., Visscher, K. M., Le Dantec, C. C., & Seitz, A. R. (2015). Alpha-band EEG activity in perceptual learning. *Journal of Vision*, *15*(10):7, 1–12, https://doi.org/10.1167/15.10.7. [PubMed] [Article]

Bell, A. J., & Sejnowski, T. J. (1995). An information-maximization approach to blind separation and blind deconvolution. *Neural Computation*, *7*, 1129–1159, https://doi.org/10.1162/neco.1995.7.6.1129.

Bogacz, R., Brown, E., Moehlis, J., Holmes, P., & Cohen, J. D. (2006). The physics of optimal decision making: A formal analysis of models of performance in two-alternative forced-choice tasks. *Psychological Review*, *113*, 700–765, https://doi.org/10.1037/0033-295X.113.4.700.

Brainard, D. H. (1997). The Psychophysics Toolbox. *Spatial Vision*, *10*, 433–436.

Britten, K. H., Shadlen, M. N., Newsome, W. T., & Movshon, J. A. (1992). The Analysis of visual motion: A comparison of neuronal and psychophysical performance. *The Journal of Neuroscience*, *12*, 4745–4765.

Brown, S. D., & Heathcote, A. (2008). The simplest complete model of choice response time: Linear ballistic accumulation. *Cognitive Psychology*, *57*, 153–178, https://doi.org/10.1016/j.cogpsych.2007.12.002.

Calhoun, V. D., Adali, T., Pearlson, G. D., & Pekar, J. J. (2001). A method for making group inferences from functional MRI data using independent component analysis. *Human Brain Mapping*, *14*, 140–151, https://doi.org/10.1002/hbm.

Chang, D. H. F., Kourtzi, Z., & Welchman, A. E. (2013). Mechanisms for extracting a signal from noise as revealed through the specificity and generality of task training. *The Journal of Neuroscience*, *33*, 10962–10971, https://doi.org/10.1523/JNEUROSCI.0101-13.2013.

Chen, N., Bi, T., Zhou, T., Li, S., Liu, Z., & Fang, F. (2015). Sharpened cortical tuning and enhanced cortico-cortical communication contribute to the long-term neural mechanisms of visual motion perceptual learning. *NeuroImage*, *115*, 17–29, https://doi.org/10.1016/j.neuroimage.2015.04.041.

Correa, N., Adali, T., & Calhoun, V. D. (2007). Performance of blind source separation algorithms for fMRI analysis using a group ICA method. *Magnetic Resonance Imaging*, *25*, 684–694, https://doi.org/10.1016/j.mri.2006.10.017.

Crist, R. E., Li, W., & Gilbert, C. D. (2001). Learning to see: Experience and attention in primary visual cortex. *Nature Neuroscience*, *4*, 519–525, https://doi.org/10.1038/87470.

Donkin, C., Averell, L., Brown, S., & Heathcote, A. (2009). Getting more from accuracy and response time data: Methods for fitting the linear ballistic accumulator. *Behavior Research Methods*, *41*, 1095–1110, https://doi.org/10.3758/BRM.41.4.1095.

Donkin, C., Brown, S., & Heathcote, A. (2011). Drawing conclusions from choice response time models: A tutorial using the linear ballistic accumulator. *Journal of Mathematical Psychology*, *55*, 140–151, https://doi.org/10.1016/j.jmp.2010.10.001.

Dosher, B. A., Jeter, P., Liu, J., & Lu, Z. (2013). An integrated reweighting theory of perceptual learning. *Proceedings of the National Academy of Sciences, USA*, *110*, 13678–13683, https://doi.org/10.1073/pnas.1312552110/-/DCSupplemental.www.pnas.org/cgi/doi/10.1073/pnas.1312552110.

Dosher, B. A., & Lu, Z. (1998). Perceptual learning reflects external noise filtering and internal noise reduction through channel reweighting. *Proceedings of the National Academy of Sciences, USA*, *95*, 13988–13993.

Dosher, B. A., & Lu, Z.-L. (2005). Perceptual learning in clear displays optimizes perceptual expertise: Learning the limiting process. *Proceedings of the National Academy of Sciences, USA*, *102*, 5286–5290, https://doi.org/10.1073/pnas.0500492102.

Dutilh, G., Vandekerckhove, J., Tuerlinckx, F., & Wagenmakers, E.-J. (2009). A diffusion model decomposition of the practice effect. *Psychonomic Bulletin & Review*, *16*, 1026–1036, https://doi.org/10.3758/16.6.1026.

Eichele, T., Debener, S., Calhoun, V. D., Specht, K., Engel, A. K., Hugdahl, K., … Ullsperger, M. (2008). Prediction of human errors by maladaptive changes in event-related brain networks. *Proceedings of the National Academy of Sciences, USA*, *105*, 6173–6178.

Engel, S. A., Glover, G. H., & Wandell, B. A. (1997). Retinotopic organization in human visual cortex

and the spatial precision of functional MRI. *Cerebral Cortex*, *7*, 181–192.

Fahle, M. (1997). Specificity of learning curvature, orientation, and vernier discriminations. *Vision Research*, *37*, 1885–1895.

Fahle, M., & Morgan, M. (1996). No transfer of perceptual learning between similar stimuli in the same retinal position. *Current Biology*, *6*, 292–297.

Fiorentini, A., & Berardi, N. (1980, September 4). Perceptual learning specific for orientation and spatial frequency. *Nature*, *287*(5777), 43–44.

Furmanski, C. S., Schluppeck, D., & Engel, S. A. (2004). Learning strengthens the response of primary visual cortex to simple patterns. *Current Biology*, *14*, 573–578, https://doi.org/10.1016/j.cub.2004.03.032.

Ghose, G. M., Yang, T., & Maunsell, J. H. R. (2002). Physiological correlates of perceptual learning in monkey V1 and V2. *Journal of Neurophysiology*, *87*, 1867–1888, https://doi.org/10.1152/jn.00690.2001.

Gilbert, C.D., Sigman, M., & Crist, R.E. (2001). The neural basis of perceptual learning. *Neuron*, *31*, 681–697.

Gold, J. I., & Shadlen, M. N. (2007). The neural basis of decision making. *Annual Review of Neuroscience*, *30*, 535–574, https://doi.org/10.1146/annurev.neuro.29.051605.113038.

Heekeren, H. R., Marrett, S., Bandettini, P. A., & Ungerleider, L. G. (2004, October 14). A general mechanism for perceptual decision-making in the human brain. *Nature*, *431*(7010), 859–862.

Heekeren, H. R., Marrett, S., & Ungerleider, L. G. (2008). The neural systems that mediate human perceptual decision making. *Nature Reviews Neuroscience*, *9*, 467–479, https://doi.org/10.1038/nrn2374.

Himberg, J., & Hyvärinen, A. (2003). ICASSO: Software for investigating the reliability of ICA estimates by clustering and visualization. *IEEE XIII Work. Neural networks signal Process* (pp. 259–268). Toulouse, France: IEEE Press.

Himberg, J., Hyvärinen, A., & Esposito, F. (2004). Validating the independent components of neuroimaging time series via clustering and visualization. *Neuroimage*, *22*, 1214–1222, https://doi.org/10.1016/j.neuroimage.2004.03.027.

Ho, T. C., Brown, S., & Serences, J. T. (2009). Domain general mechanisms of perceptual decision making in human cortex. *The Journal of Neuroscience*, *29*, 8675–8687, https://doi.org/10.1523/JNEUROSCI.5984-08.2009.

Hol, K., & Treue, S. (2001). Different populations of neurons contribute to the detection and discrimination of visual motion. *Vision Research*, *41*(6), 685–689, https://doi.org/10.1016/S0042-6989(00)00314-X.

Hua, T., Bao, P., Huang, C.-B., Wang, Z., Xu, J., Zhou, Y., Lu, Z.-L. (2010). Perceptual learning improves contrast sensitivity of V1 neurons in cats. *Current Biology*, *20*, 887–894, https://doi.org/10.1016/j.cub.2010.03.066.

Huang, X., Lu, H., Tjan, B. S., Zhou, Y., & Liu, Z. (2007). Motion perceptual learning: When only task-relevant information is learned. *Journal of Vision*, *7*(10):14, 1–10, https://doi.org/10.1167/7.10.14. [PubMed] [Article]

Huk, A. C., Dougherty, R. F., & Heeger, D. J. (2002). Retinotopy and functional subdivision of human areas MT and MST. *The Journal of Neuroscience*, *22*, 7195–7205.

Hung, S., & Seitz, A. R. (2014). Prolonged training at threshold promotes robust retinotopic specificity in perceptual learning. *The Journal of Neuroscience*, *34*, 8423–8431, https://doi.org/10.1523/JNEUROSCI.0745-14.2014.

Jazayeri, M., & Movshon, J. A. (2007, April 19). A new perceptual illusion reveals mechanisms of sensory decoding. *Nature*, *446*(7138), 912–915, https://doi.org/10.1038/nature05739.

Jehee, J. F. M., Ling, S., Swisher, J. D., van Bergen, R. S., & Tong, F. (2012). Perceptual learning selectively refines orientation representations in Early Visual Cortex. *The Journal of Neuroscience*, *32*, 16747–16753, https://doi.org/10.1523/JNEUROSCI.6112-11.2012.

Jia, K., & Li, S. (2017). Motion direction discrimination training reduces perceived motion repulsion. *Attention, Perception & Psychophysics*, *79*, 878–887, https://doi.org/10.3758/s13414-016-1261-x.

Kahnt, T., Grueschow, M., Speck, O., & Haynes, J.-D. (2011). Perceptual learning and decision-making in human medial frontal cortex. *Neuron*, *70*(3), 549–559, https://doi.org/10.1016/j.neuron.2011.02.054.

Karni, A., & Sagi, D. (1991). Where practice makes perfect in texture discrimination: Evidence for primary visual cortex plasticity. *Proceedings of the National Academy of Sciences, USA*, *88*, 4966–4970.

Kayser, A. S., Buchsbaum, B. R., Erickson, D. T., & Esposito, M. D. (2010). The functional anatomy of a perceptual decision in the human brain. *Journal of Neurophysiology*, *103*, 1179–1194, https://doi.org/10.1152/jn.00364.2009.

Kelly, S. P., & O'Connell, R. G. (2013). Internal and external influences on the rate of sensory evidence accumulation in the human brain. *The Journal of*

Neuroscience, *33*, 19434–19441, https://doi.org/10.1523/JNEUROSCI.3355-13.2013.

Kim, K., & Shadlen, M. N. (1999). Neural correlates of a decision in the dorsolateral prefrontal cortex of the macaque. *Nature Neuroscience*, *2*(2), 176–185, https://doi.org/10.1038/5739.

Kourtzi, Z., & Kanwisher, N. (2000) . Cortical regions involved in perceiving object shape. *The Journal of Neuroscience*, *20*, 3310–3318.

Krajbich, I., Armel, C., & Rangel, A. (2010). Visual fixations and the computation and comparison of value in simple choice. *Nature Neuroscience*, *13*, 1292–1298, https://doi.org/10.1038/nn.2635.

Law, C.-T., & Gold, J.I (2009). Reinforcement learning can account for associative and perceptual learning on a visual-decision task. *Nature Neuroscience*, *12*, 655–663, https://doi.org/10.1038/nn.2304.

Law, C.-T., & Gold, J. I (2008). Neural correlates of perceptual learning in a sensory-motor, but not a sensory, cortical area. *Nature Neuroscience*, *11*, 505–513, https://doi.org/10.1038/nn2070.

Liang, J., Zhou, Y., Fahle, M., & Liu, Z. (2015a). Limited transfer of long-term motion perceptual learning with double training. *Journal of Vision*, *15*(10):1, 1–9, https://doi.org/10.1167/15.10.1. [PubMed] [Article]

Liang, J., Zhou, Y., Fahle, M., & Liu, Z. (2015b). Specificity of motion discrimination learning even with double training and staircase. *Journal of Vision*, *15*(10):3, 1–10, https://doi.org/10.1167/15.10.3. [PubMed] [Article]

Liu, C. C., & Watanabe, T. (2012). Accounting for speed- accuracy tradeoff in perceptual learning. *Vision Research*, *61*, 107–114, https://doi.org/10.1016/j.visres.2011.09.007.

Liu, T., & Pleskac, T. J., 2011. Neural correlates of evidence accumulation in a perceptual decision task. *Journal of Neurophysiology*, *106*(5), 2383–2398, https://doi.org/10.1152/jn.00413.2011.

Maniglia, M., & Seitz, A. R. (2018). Towards a whole brain model of Perceptual Learning. *Current Opinion in Behavioral Sciences*, *20*, 47–55, https://doi.org/10.1016/j.cobeha.2017.10.004.

McGovern, D. P., Roach, N. W., & Webb, B. S. (2012). Perceptual learning reconfigures the effects of visual adaptation. *The Journal of Neuroscience*, *32*, 13621–13629, https://doi.org/10.1523/JNEUROSCI.1363-12.2012.

Mckeefry, D. J., Burton, M. P., Vakrou, C., Barrett, B. T., & Morland, A. B. (2008). Induced deficits in speed perception by transcranial magnetic stimulation of human cortical areas V5/MT+ and V3A. *The Journal of Neuroscience*, *28*, 6848–6857, https://doi.org/10.1523/JNEUROSCI.1287-08.2008.

Mollon, J. D., & Danilova, M. V. (1996). Three remarks on perceptual learning. *Spatial Vision*, *10*, 51–58.

Mukai, I., Kim, D., Fukunaga, M., Japee, S., Marrett, S., & Ungerleider, L. G. (2007). Activations in visual and attention-related areas predict and correlate with the degree of perceptual learning. *The Journal of Neuroscience*, *27*, 11401–11411, https://doi.org/10.1523/JNEUROSCI.3002-07.2007.

Na, R., Bi, T., Tjan, B. S., Liu, Z., & Fang, F. (2018). Effect of task difficulty on blood-oxygen-level-dependent signal: A functional magnetic resonance imaging study in a motion discrimination task. *PLoS One*, *13*, 1–19, https://doi.org/10.1371/journal.pone.0199440.

Pelli, D. G., 1997. The VideoToolbox software for visual psychophysics: Transforming numbers into movies. *Spatial Vision*, *10*, 437–442.

Petrov, A. A., Dosher, B. A., & Lu, Z. (2005). The dynamics of perceptual learning: An incremental Rreweighting model. *Psychological Review*, *112*, 715–743, https://doi.org/10.1037/0033-295X.112.4.715.

Petrov, A. A., Van Horn, N. M., & Ratcliff, R. (2011). Dissociable perceptual-learning mechanisms revealed by diffusion-model analysis. *Psychonomic Bulletin & Review*, *18*, 490–497, https://doi.org/10.3758/s13423-011-0079-8.

Raiguel, S., Vogels, R., Mysore, S. G., & Orban, G. A. (2006). Learning to see the difference specifically alters the most informative V4 neurons. *The Journal of Neuroscience*, *26*(24), 6589–6602, https://doi.org/10.1523/JNEUROSCI.0457-06.2006.

Ratcliff, R., & McKoon, G., 2008. The diffusion decision model: Theory and data for two-choice decision tasks. *Neural Computation*, *20*, 873–922, https://doi.org/10.1162/neco.2008.12-06-420.

Romo, R., Hernandez, A., & Zainos, A. (2004). Neuronal correlates of a perceptual decision in ventral premotor cortex. *Neuron*, *41*(1), 165–173, https://doi.org/S0896627303008171.

Sagi, D., & Tanne, D., 1994. Perceptual learning: Learning to see. *Current Opinion in Neurobiology*, *4*, 195–199.

Salzman, C. D., Murasugi, C. M., Britten, K. H., & Newsome, W. T. (1992). Microstimulation in visual area MT: Effects on direction discrimination performance. *The Journal of Neuroscience*, *12*, 2331–2355.

Sasaki, Y., Nanez, J. E., & Watanabe, T. (2010). Advances in visual perceptual learning and plasticity. *Nature Reviews Neuroscience*, *11*, 53–60, https://doi.org/10.1038/nrn2737.

Schoups, A., Vogels, R., Qian, N., & Orban, G. (2001, August 2). Practising orientation identification improves orientation coding in V1 neurons. *Nature*, *412*(6846), 549–553.

Sereno, M. I., Dale, A. M., Reppas, J. B., Kwong, K. K., Belliveau, J. W., Brady, T. J., ... & Tootell, R. B. H. (1995, May 12). Borders of multiple visual areas in humans revealed by functional magnetic resonance imaging. *Science*, *268*(5212), 889–893.

Shadlen, M. N., & Newsome, W. T., 2001. Neural basis of a perceptual decision in the parietal cortex (area LIP) of the rhesus monkey. *Journal of Neurophysiology*, *86*, 1916–1936.

Shibata, K., Chang, L.-H., Kim, D., Nanez, J. E., Kamitani, Y., Watanabe, T., & Sasaki, Y. (2012). Decoding reveals plasticity in V3A as a result of motion perceptual learning. *PLoS One*, *7*, 1–7, https://doi.org/10.1371/journal.pone.0044003.

Shibata, K., Sagi, D., & Watanabe, T. (2014). Two-stage model in perceptual learning: Toward a unified theory. *Annals of the New York Academy of Science*, *1316*, 18–28, https://doi.org/10.1111/nyas.12419.

Shibata, K., Sasaki, Y., Kawato, M., & Watanabe, T. (2016). Neuroimaging evidence for 2 types of plasticity in association with visual perceptual learning. *Cerebral Cortex*, *26*, 3681–3689, https://doi.org/10.1093/cercor/bhw176.

Smith, P. L., & Ratcliff, R. (2004). Psychology and neurobiology of simple decisions. *Trends in Neurosciences*, *27*, 161–168, https://doi.org/10.1016/j.tins.2004.01.006.

Stephan, K. E., Penny, W. D., Daunizeau, J., Moran, R. J., & Friston, K. J. (2009). Bayesian model selection for group studies. *Neuroimage*, *46*, 1004–1017, https://doi.org/10.1016/j.neuroimage.2009.03.025.

Szpiro, S. F. A., Spering, M., & Carrasco, M. (2014). Perceptual learning modifies untrained pursuit eye movements. *Journal of Vision*, *14*(8):8, 1–13, https://doi.org/10.1167/14.8.8. [PubMed] [Article]

Teich, A. F., & Qian, N. (2003). Learning and adaptation in a recurrent model of V1 orientation selectivity. *Journal of Neurophysiology*, *89*, 2086–2100, https://doi.org/10.1152/jn.00970.2002.

Thompson, B., Tjan, B. S., & Liu, Z. (2013). Perceptual learning of motion direction discrimination with suppressed and unsuppressed MT in humans: An fMRI study. *PLoS One*, *8*, e53458, https://doi.org/10.1371/journal.pone.0053458.

Tootell, R. B. H., Mendola, J. D., Hadjikhani, N. K., Ledden, P. J., Liu, A. K., Reppas, J. B., ... Dale, A. M. (1997). Functional analysis of V3A and related areas in human visual cortex. *The Journal of Neuroscience*, *17*, 7060–7078.

van Maanen, L., Brown, S. D., Eichele, T., Wagenmakers, E.-J., Ho, T., Serences, J., & Forstmann, B. U. (2011). Neural correlates of trial-to-trial fluctuations in response caution. *The Journal of Neuroscience*, *31*, 17488–17495, https://doi.org/10.1523/JNEUROSCI.2924-11.2011.

Watanabe, T., & Sasaki, Y. (2015). Perceptual learning: Toward a comprehensive theory. *Annual Review of Psychology*, *66*, 1–25, https://doi.org/10.1146/annurev-psych-010814-015214.

Xiao, L.-Q., Zhang, J.-Y., Wang, R., Klein, S. A., Levi, D. M., & Yu, C. (2008). Complete transfer of perceptual learning across retinal locations enabled by double training. *Current Biology*, *18*, 1922–1926, https://doi.org/10.1016/j.cub.2008.10.030.

Yan, Y., Rasch, M. J., Chen, M., Xiang, X., Huang, M., Wu, S., & Li, W. (2014). Perceptual training continuously refines neuronal population codes in primary visual cortex. *Nature Neuroscience*, *17*, 1380–1389, https://doi.org/10.1038/nn.3805.

Yang, F., Wu, Q., & Li, S. (2014). Learning-induced uncertainty reduction in perceptual decisions is task-dependent. *Frontiers in Human Neuroscience*, *8*, 1–10, https://doi.org/10.3389/fnhum.2014.00282.

Yang, T., & Maunsell, J. H. R., 2004. The effect of perceptual learning on neuronal responses in monkey visual area V4. *The Journal of Neuroscience*, *24*(7), 1617–1626, https://doi.org/10.1523/JNEUROSCI.4442-03.2004.

Yotsumoto, Y., Watanabe, T., & Sasaki, Y. (2008). Different dynamics of performance and brain activation in the time course of perceptual learning. *Neuron*, *57*, 827–833, https://doi.org/10.1016/j.neuron.2008.02.034.

Yu, Q., Zhang, P., Qiu, J., & Fang, F. (2016). Perceptual learning of contrast detection in the human lateral geniculate nucleus. *Current Biology*, *26*, 3176–3182, https://doi.org/10.1016/j.cub.2016.09.034.

Zamboni, E., Ledgeway, T., McGraw, P. V., & Schluppeck, D. (2016). Do perceptual biases emerge early or late in visual processing? Decision-biases in motion perception. *Proceedings of the Royal Society B: Biological Sciences*, *283*, 1–9, https://doi.org/10.1098/rspb.2016.0263.

Zhang, J. (2012). The effects of evidence bounds on

decision-making: Theoretical and empirical developments. *Frontiers in Psychology*, *3*, 1–19, https://doi.org/10.3389/fpsyg.2012.00263.

Zhang, J.-Y., Zhang, G.-L., Xiao, L.-Q., Klein, S. A., Levi, D. M., & Yu, C. (2010). Rule-based learning explains visual perceptual learning and its specificity and transfer. *The Journal of Neuroscience*, *30*, 12323–12328, https://doi.org/10.1523/JNEUROSCI.0704-10.2010.

Zhang, J., Hughes, L. E., & Rowe, J. B. (2012). Selection and inhibition mechanisms for human voluntary action decisions. *Neuroimage*, *63*, 392–402, https://doi.org/10.1016/j.neuroimage.2012.06.058.

Zhang, J., & Rowe, J. B. (2014). Dissociable mechanisms of speed-accuracy tradeoff during visual perceptual learning are revealed by a hierarchical drift-diffusion model. *Frontiers in Neuroscience*, *8*, 1–13, https://doi.org/10.3389/fnins.2014.00069.

Zhang, J., & Yu, C. (2016). The transfer of motion direction learning to an opposite direction enabled by double training: A reply to Liang et al. (2015). *Journal of Vision*, *16*(3):29, 1–4, https://doi.org/10.1167/16.3.29. [PubMed] [Article]